SUPPLEMENTARY INFORMATION

Decoupling ionic and electronic pathways in low-dimensional hybrid conductors

Yubing Zhou,[1,†] Chaoji Chen,[1,†] Xin Zhang,[1,†] Dapeng Liu,[1] Lisha Xu,[1] Jiaqi Dai,[1] Sz-Chian Liou,[2] Yilin Wang,[1] Claire Li, [1] Hua Xie,[1] Qingyun Wu,[1] Bob Foster,[3] Teng Li,[4] Robert M. Briber,[1] Liangbing Hu[1*]

1. Department of Materials Science and Engineering, University of Maryland, College Park, Maryland, 20742
2. Advanced Imaging and Microscopy (AIM) Lab of Nano Center, University of Maryland, College Park, 20742
3. Trinity Industries, Inc., Dallas, Texas, 75207.
4. Department of Mechanical Engineering, University of Maryland, College Park, MD 20742.

[*] Email: binghu@umd.edu

†These authors contributed equally to this work.

Methods

Preparation process of graphite-NFC slurry

NFC fibers with negatively charged carboxyl groups were produced by (2,2,6,6-tetramethylpiperidin-1-yl)oxidanyl (TEMPO) oxidation. A total of 5 g of Kraft bleached hardwood (Eucalyptus) pulp was suspended in 250 mL deionized water containing 0.5 mmol TEMPO (Sigma-Aldrich, 99%) and 5 mmol NaBr (Sigma-Aldrich, ⩾99.99%). The TEMPO mediated oxidation is initiated with the addition of 25 mmol NaClO. The pH is maintained at 10.0 with 1 mol/L NaOH solution. The whole oxidation process is maintained under stirring (IKA RW20 digital mixer) for 2-3 h. The resulting pulp was then washed by filtration and stored at 4 °C for further analysis and treatment. The diameter of the resulting fibers was further reduced by mechanical treatment in a microfluidizer (M-110EH Microfluidizer Processor) at pressures of 20,000 psi.

To make graphite-NFC slurry with a mass ratio of 1:1, commercial graphite powder (Asbury Carbons 3061) and obtained NFC solution were mixed together with a solid mass ratio of 1:1 for graphite to NFC. The dispersion process was performed using a Vibra-Cell ultrasonic liquid processor for 5 min, and then bath sonicated for 15 min (FS110D, Fisher Scientific). After sonication, the graphite flakes were well dispersed in the NFC solution. More details about graphite-NFC slurry making process can be found in our previous article [1].

3D printing

3D printing fabrication was conducted using a benchtop robot (Fisnar F4200n), which was controlled by programmed procedures. The graphite-NFC slurry was placed into a syringe tube with a 305 μm tip diameter for the printing process. An air-driven fluid dispenser (DSP501N, Fisnar) provided appropriate pressure (30-50 psi) to extrude the slurry onto a glass slide. After

printing, the samples of various geometries were transferred into a constant temperature humidity chamber (LHS-150HC-II, set to 40 °C, 40% RH) for 3 h to remove water.

Characterization

The graphite-NFC composite was embedded in epoxy and microtomed at room temperature under either dry or wet conditions with a diamond knife. The section was ~100 nm thick. TEM observation was conducted with a JEOL JEM-2100 TEM at 200kV acceleration voltage and equipped with a Gatan Tridiem 863 GIF (Gatan Imaging Filter) system. All the high resolution TEM images were recorded under the Scherzer defocus condition. SEM images were taken with a Hitachi SU-70 Schottky field emission gun scanning electron microscope (2-5 kV, depending on the sample state). All samples were coated by gold sputtering for 90 s prior to observation. The Zeta potential was determined using a Zetasizer Nano ZS90. TGA data were collected with a TA instrument (SDT650) from room temperature to 800 °C at a heating rate of 3 °C/min in air atmosphere.

Conductivity Measurement of the ionic conductors

The dry and fully swollen graphite-NFC films were cut into a rectangular shape. Then the films were sealed in hard epoxy to remain the thickness unchanged. The two ends of the film were exposed to ensure good contact with the electrodes. The as-made nanofluidic devices were soaked in different concentrations of NaCl solution for conductivity measurements. At each concentration, the devices were soaked more than 24 h to reach equilibrium. The conductivity measurements were conducted with a BioLogic VMP3 potentiostat. Two Ag/AgCl electrodes were attached to the two ends of the nanofluidic device as the electrodes. I-V curves of ionic conductors were recorded at various electrolyte concentrations from 10^{-6} M to 1 M.

References

1. Zhou, Y.; Chen, C.; Zhu, S.; Sui, C.; Wang, C.; Kuang, Y.; Ray, U.; Liu, D.; Brozena, A.; Leiste, U. H.; Quispe, N.; Guo, H.; Vellore, A.; Bruck, H. A.; Martini, A.; Foster, B.; Lou, J.; Li, T.; Hu, L. A printed, recyclable, ultra-strong, and ultra-tough graphite structural material. *Mater. Today* **2019** DOI:10.1016/j.mattod.2019.03.016.

Supplementary figures

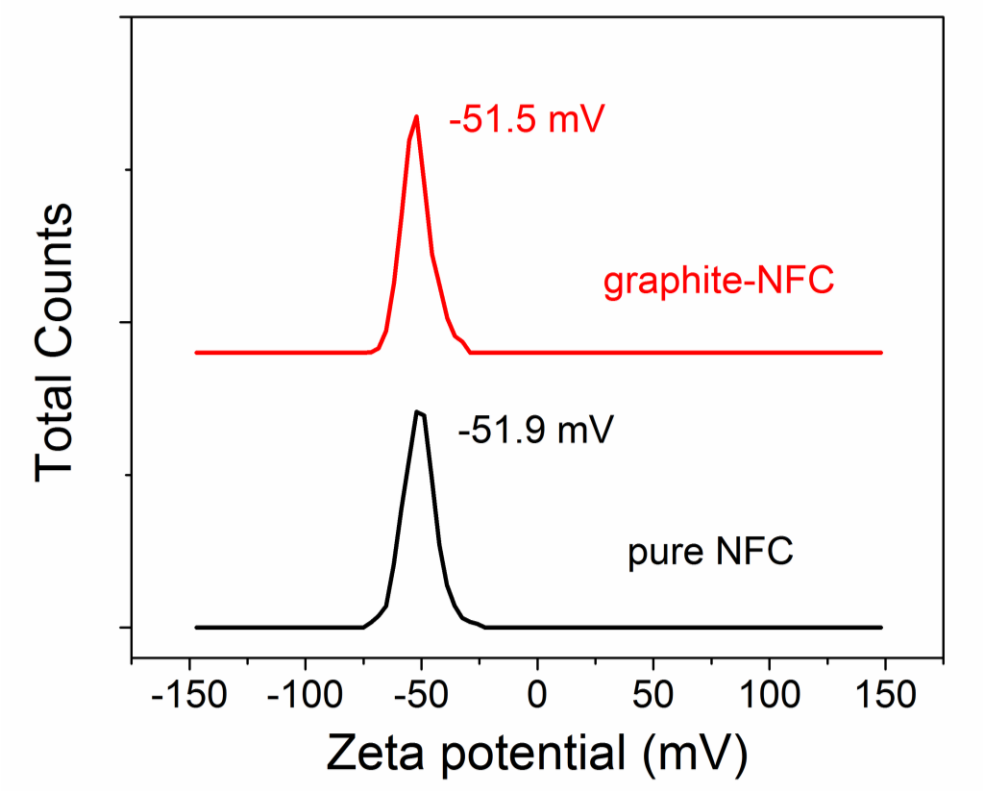

Figure S1. Zeta potential of pure NFC and graphite-NFC slurry.

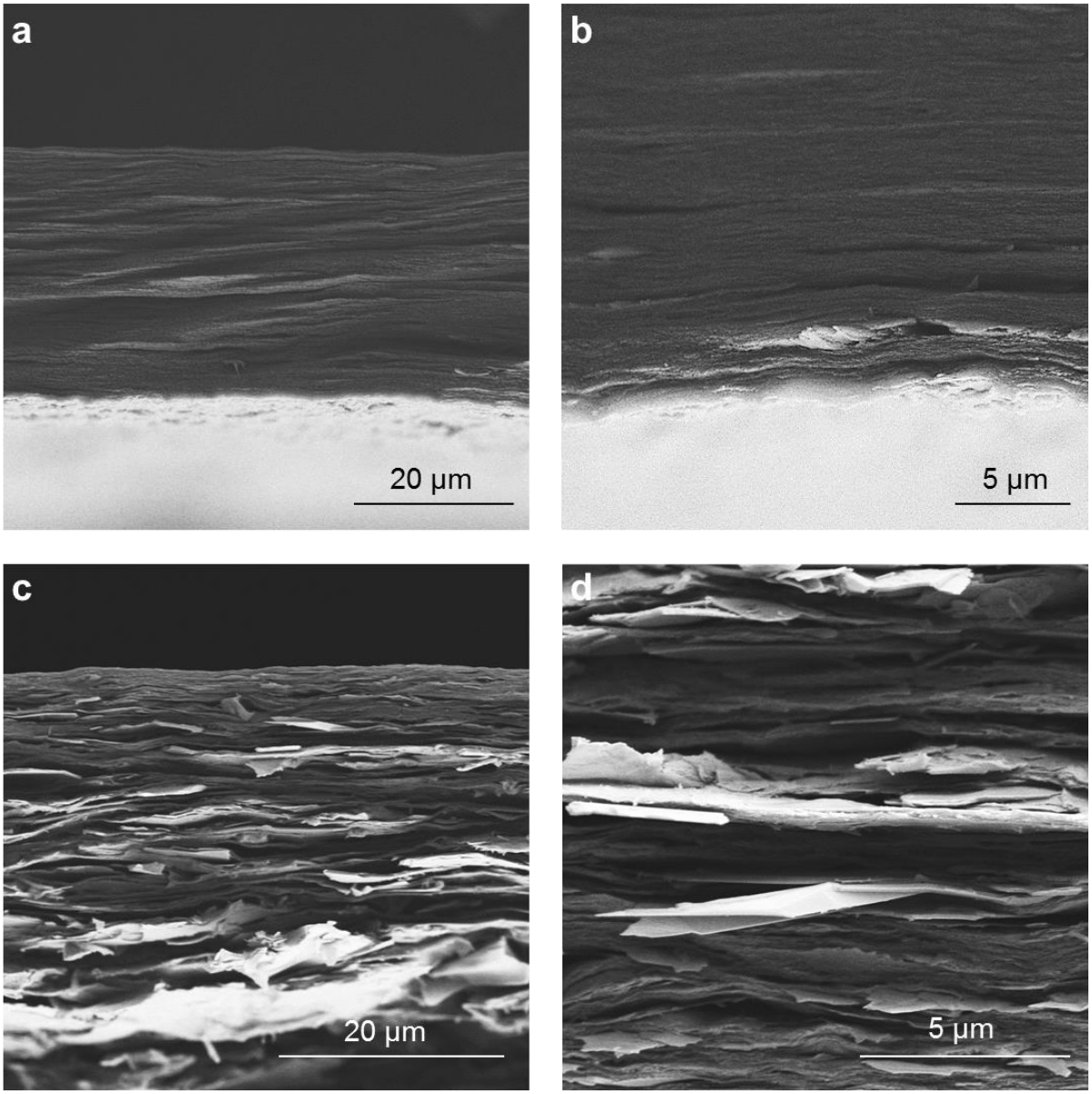

Figure S2. (a,b) Cross-sectional SEM images of pure NFC paper, and (c,d) the graphite-NFC membrane.

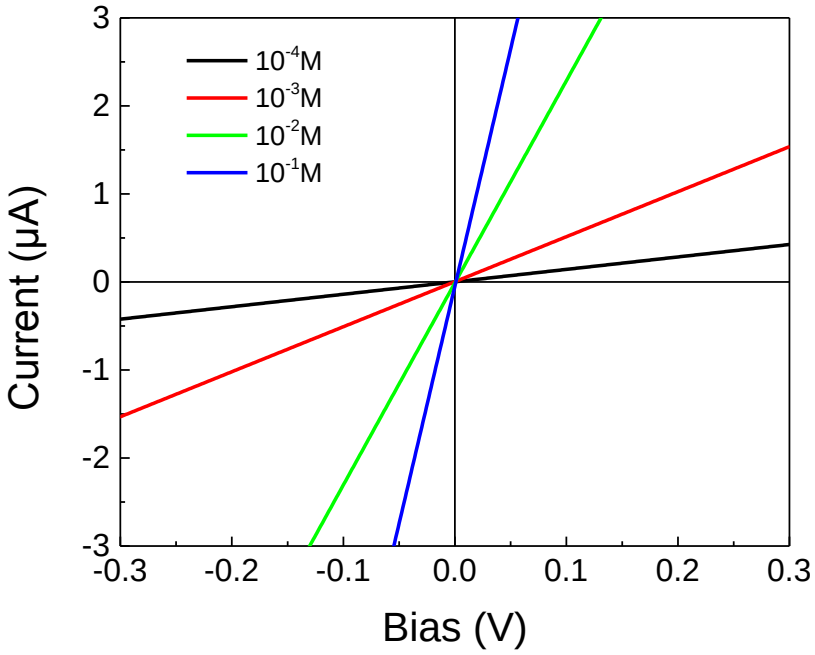

Figure S3. Representative I-V curves of the confined graphite-NFC membrane at different NaCl concentrations.

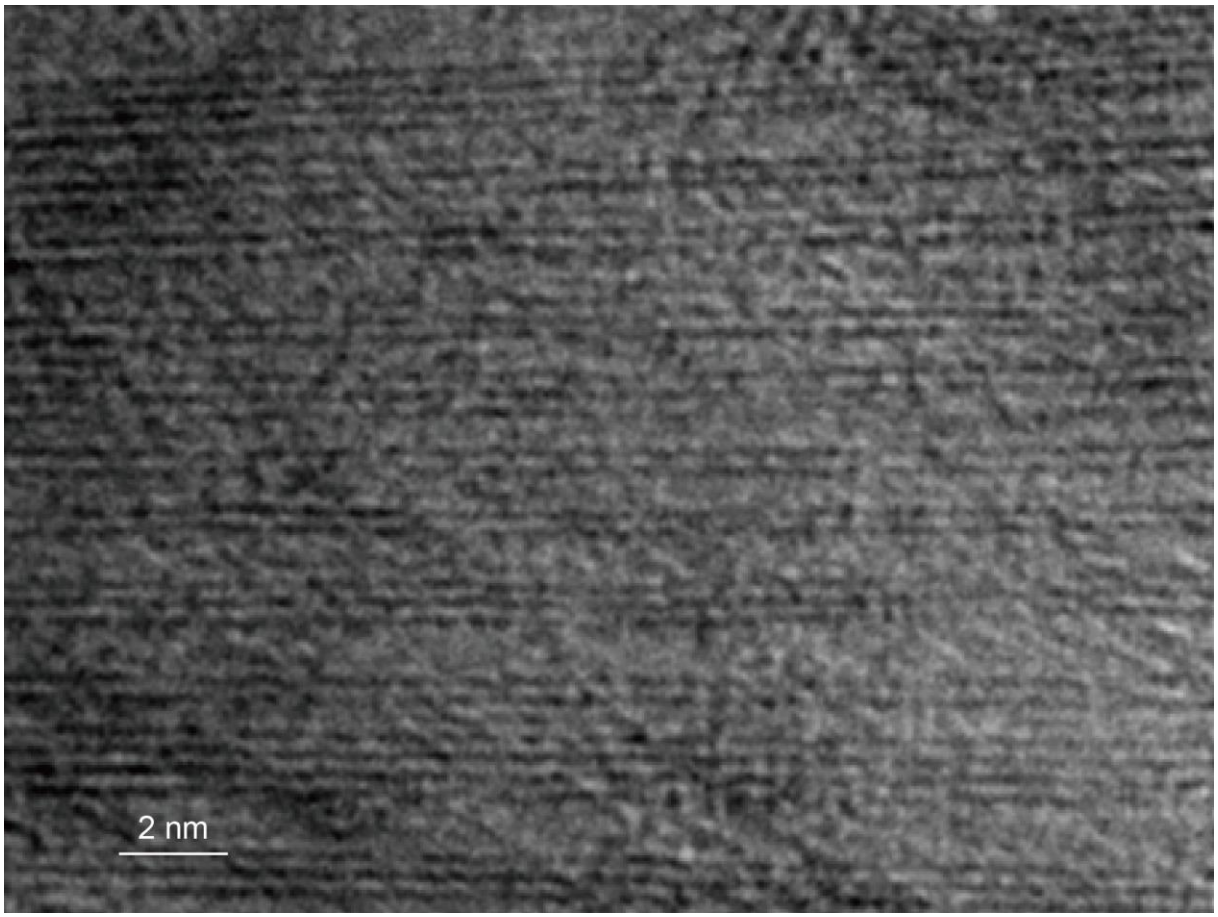

Figure S4. High resolution TEM image of the exfoliated graphite flake shown in Figure 4c.

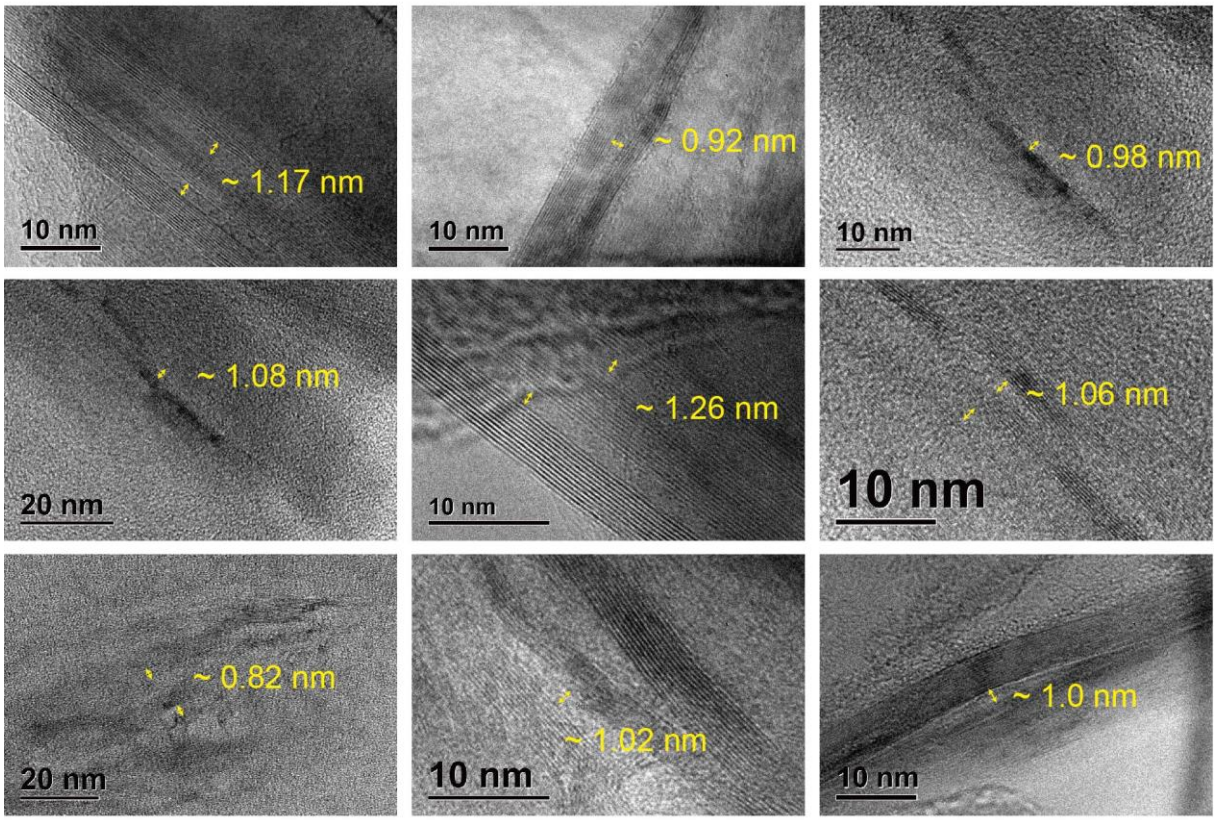

Figure S5. High resolution TEM images of ultrathin sections of graphite-NFC membranes in confined hydrated state embedded in epoxy. The actual spacing between the flakes can be observed clearly.

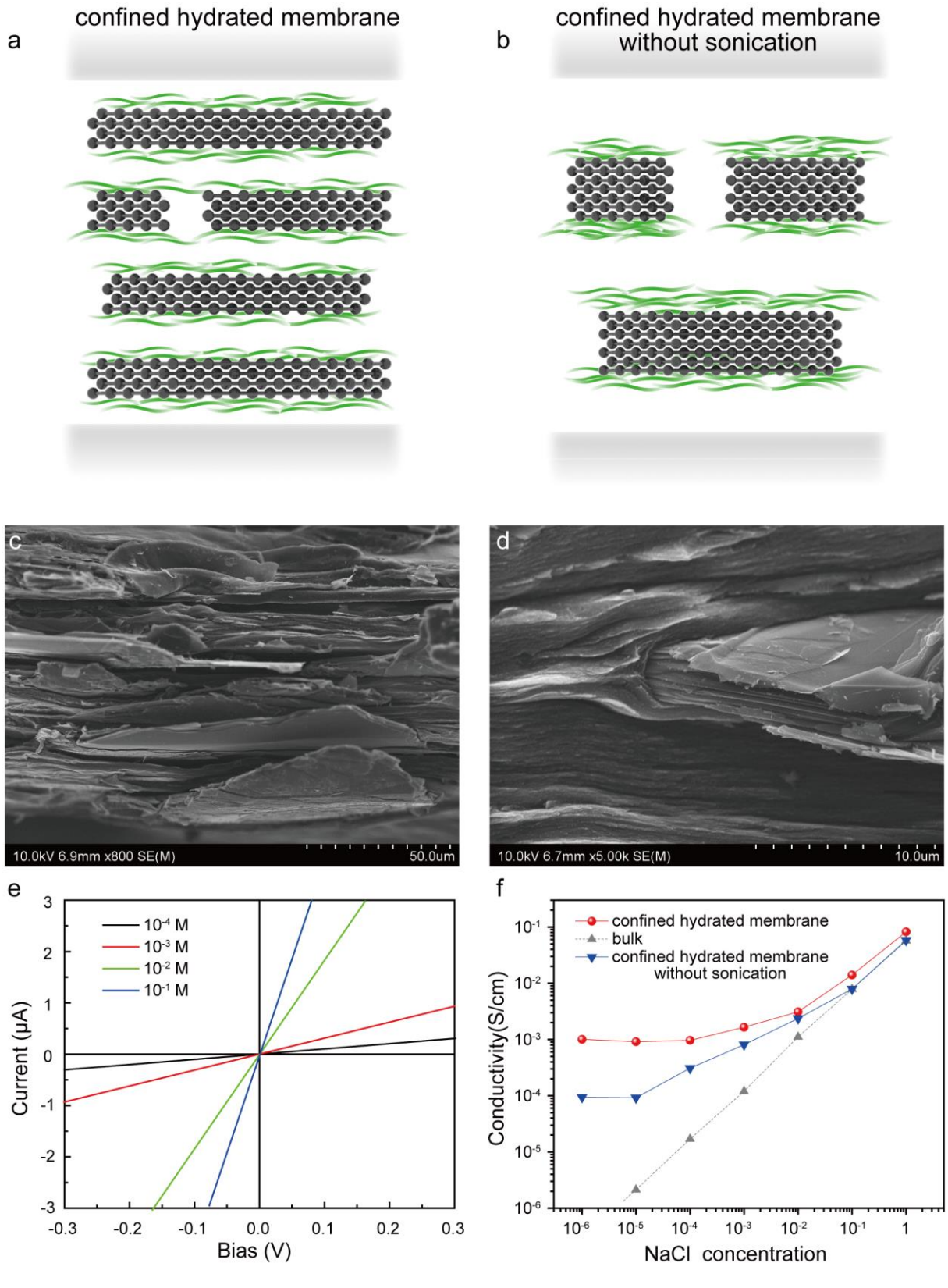

Figure S6. (a, b) Schematics of the nanofluidic channels of the graphite-NFC membrane (a) with sonication and (b) without sonication. (c, d) Cross-sectional SEM image of the graphite-NFC membrane made without sonication. (e) Representative I-V curves of the confined hydrated graphite-NFC membrane without sonication at different NaCl concentrations. (f) The ionic conductivity as a function of electrolyte concentration at different NaCl concentrations. The blue and red lines are the ionic conductivities of the confined hydrated graphite-NFC membranes with and without sonication, respectively.

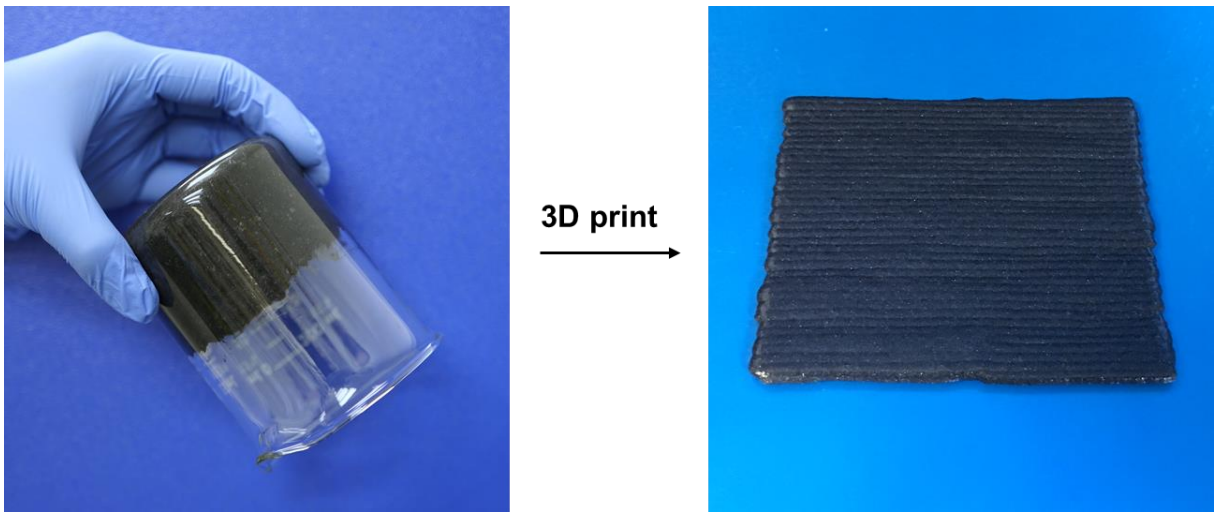

Figure S7. The graphite-NFC slurry with a solid content of 20 wt.% shows ideal gel-like behavior and superior filament shape retention after extrusion by 3D printing.

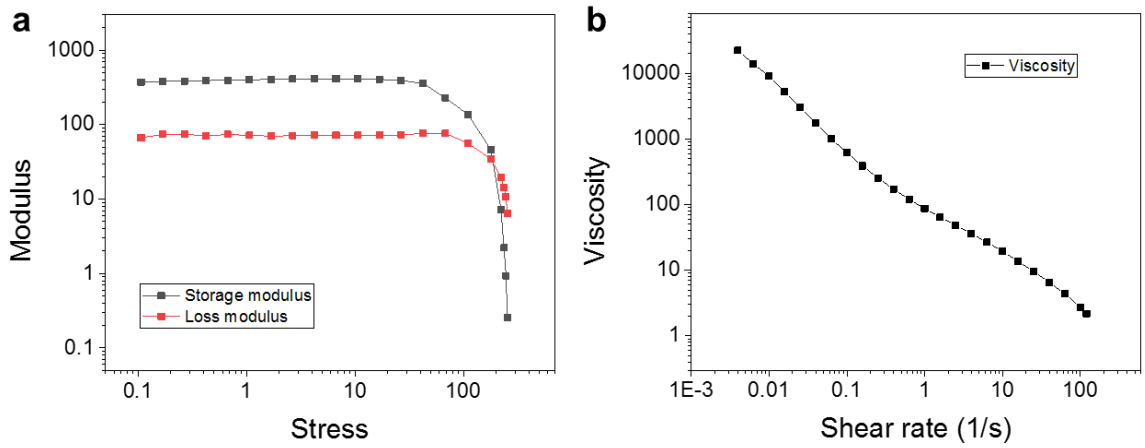

Figure S8. (a) Storage modulus and loss modulus as a function of shear stress for graphite-NFC slurry. Typical viscoelastic property is suitable for extrusion-based 3D printing. (b) Apparent viscosity as a function of shear rate for graphite-NFC slurry.

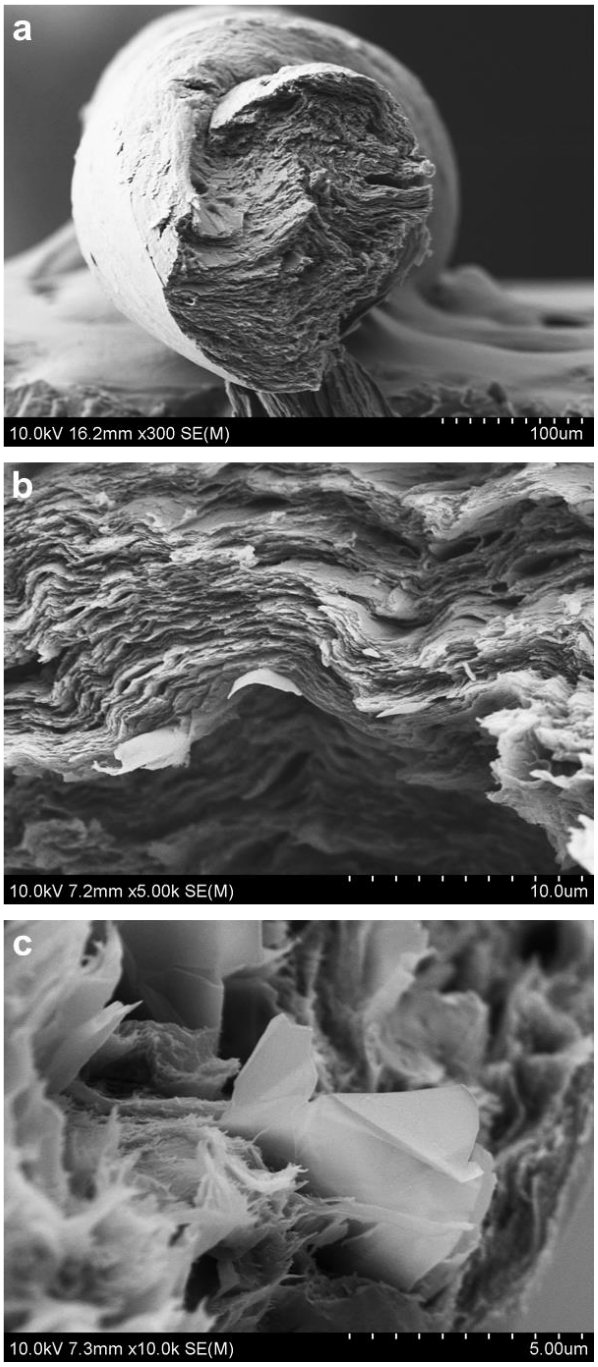

Figure S9. (a) Low-magnification and (b, c) high-magnification cross-section SEM images of the graphite-NFC fiber.

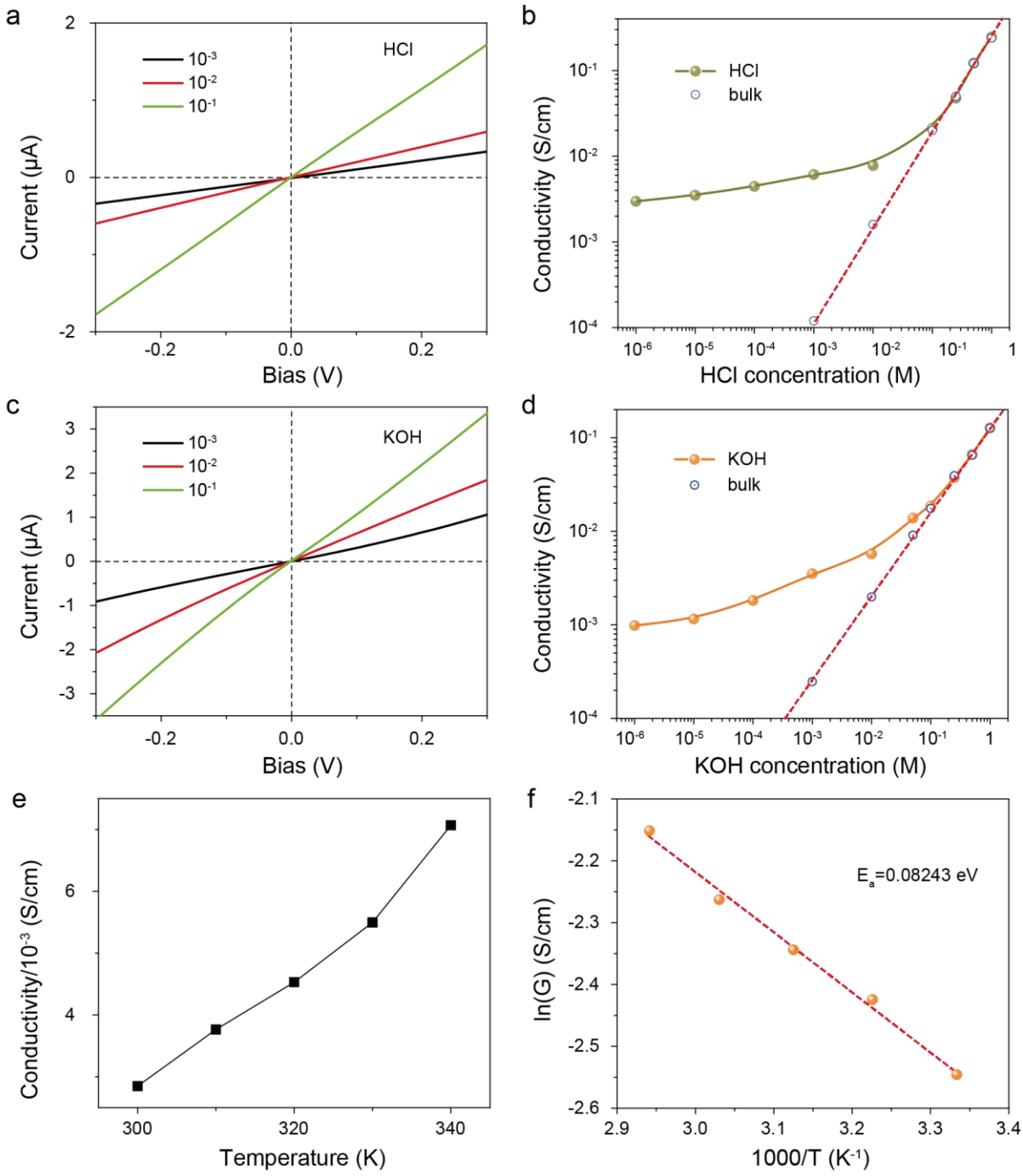

Figure S10. Ionic conductivity tests of graphite-NFC membrane-based nanofluidic devices were carried out at various HCl or KOH concentrations (up to 1 M) respectively. (a) I−V curves obtained at HCl concentrations of 0.001, 0.01, and 0.1 M. (b) Ionic conductivity as a function of the HCl concentration. (c) I−V curves obtained at KOH concentrations of 0.001, 0.01, and 0.1 M. (d) Ionic

conductivity as a function of the KOH concentration. (e) Ionic conductivity of the graphite-CNF film at different temperatures. (f) Arrhenius plot of the conductance (ln(G)) vs. inverse temperature (1000/T) for the graphite-NFC film.

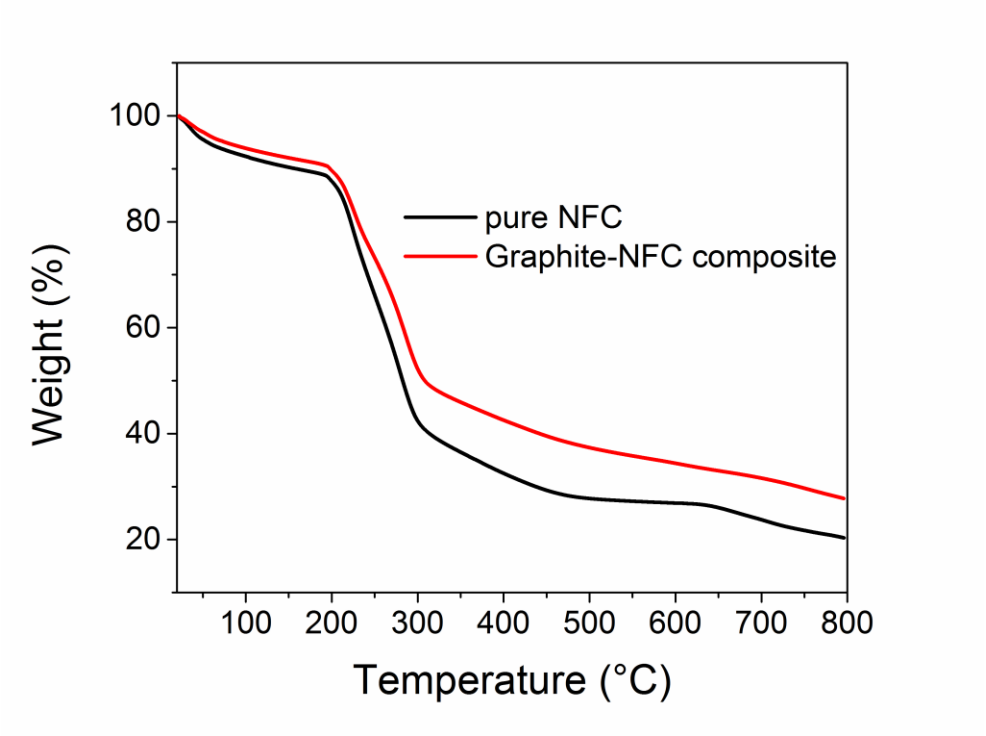

Figure S11. Thermogravimetric curves showing the thermal degradation of graphite-NFC composite and pure NFC.